

Nonspecific Protein–DNA Interactions: Complexation of α -Chymotrypsin with a Genomic DNA

S. Shankara Narayanan and Samir Kumar Pal*

Unit for Nano Science & Technology, Department of Chemical, Biological & Macromolecular Sciences, S. N. Bose National Centre for Basic Sciences, Block JD, Sector III, Salt Lake, Kolkata 700 098, India

Received December 11, 2006. In Final Form: March 15, 2007

In this contribution, we report studies on nonspecific protein–DNA interactions of an enzyme protein bovine pancreatic α -chymotrypsin (CHT) with genomic DNA (from salmon testes) using two biologically common fluorescent probes: 1-anilino-naphthalene-8-sulfonate (ANS) and 2,6-*p*-toluidino-naphthalene sulfonate (TNS). TNS molecules that are nonspecifically bound to positively charged basic residues at the surface sites, not in the hydrophobic cavities of the protein, are preferentially displaced upon complexation of TNS-labeled CHT with DNA. The time-resolved fluorescence anisotropy of TNS molecules bound to hydrophobic cavities/clefts of CHT reveals that global tumbling motion of the protein is almost frozen in the protein–DNA complex. A control study on TNS-labeled human serum albumin (HSA) upon interaction with DNA clearly indicates that the ligands in the deep pockets of the protein cannot be displaced by interaction with DNA. We have also found that ANS, which binds to a specific surface site of CHT, is not displaced by DNA. The intactness of the ANS binding in CHT upon complexation with DNA offers the opportunity to measure the distance between the ANS binding site and the contact point of the ethidium bromide (EB)-labeled DNA using the Förster resonance energy transfer (FRET) technique. Enzymatic activity studies on CHT on a substrate (Ala-Ala-Phe 7-amido-4-methyl coumarin) reveal that the active site of the enzyme remains open for the substrate even in the protein–DNA complex. Circular dichroism (CD) studies on CHT upon complexation with DNA confirm the structural integrity of CHT in the complex. Our studies have attempted to explore an application of nonspecific protein–DNA interactions in the characterization of ligand binding of a protein in solution.

Introduction

Protein–DNA interactions play a pivotal role in many vital processes such as the regulation of gene expression, DNA replication and repair, and packaging. The most important biochemical interactions in protein–DNA complexes are van der Waals, hydrogen bonding, and water-mediated interactions.¹ About two-thirds of all interactions are nonspecific and are made with the sugar–phosphate backbone of DNA, leaving one-third of all interactions for specificity.² Nonspecific protein–DNA interactions generally involve a highly dynamic process in which a protein can bind to and readily move between multiple overlapping binding sites on the DNA with comparable affinity. The electrostatic interactions between proteins and DNA play a major role in the binding of protein to nonspecific sequences of DNA.^{3,4} In sequence-specific DNA-binding proteins, nonspecific interactions may serve to enhance the specific association rate by initially binding to DNA anywhere along the chain, followed by intramolecular translocation to the specific binding site.^{4–6} Most, if not all, proteins that interact with specific sites also bind nonspecifically to DNA with appreciable affinity.^{7,8} Some proteins only bind DNA nonspecifically.^{9,10} One classical example is histone, which plays a central role in DNA packaging

in the form of chromatin.¹⁰ Thus, nonspecific protein–DNA interaction is an important intermediate step in the process of sequence-specific recognition and binding.¹¹

Here, we report our studies on nonspecific protein–DNA interactions using two different biologically relevant probes: 1-anilino-naphthalene-8-sulfonate (ANS)¹² and 2,6-*p*-toluidino-naphthalene sulfonate (TNS)¹³ bound to the enzyme protein α -chymotrypsin (CHT) upon complexation with genomic salmon sperm DNA (SS DNA). These probes are essentially nonfluorescent in aqueous solution but fluoresce strongly both in organic solvents and when bound to certain native proteins.^{13–16} The anionic TNS, one of the most popular biological probes, binds mainly with the positively charged basic residues of a protein by noncovalent electrostatic interactions; there is also the possibility for TNS to bind with a hydrophobic domain.^{17–19} However, ANS, a well-known solvation probe,^{20,21} binds selectively to the native state of certain proteins and enzymes in their hydrophobic as well as polar sites.^{22,23} The binding of ANS and TNS to proteins and consequent changes in their fluorescence have been studied in detail by many groups.^{22,24,25}

* Corresponding author. E-mail: skpal@bose.res.in. Fax: 91 33 2335 3477.

(1) Luscombe, N. M.; Laskowski, R. A.; Thornton, J. M. *Nucleic Acids Res.* **2001**, *29*, 2860.
 (2) Steffen, N. R.; Murphy, S. D.; Toller, L.; Hatfield, G. W.; Lathrop, R. H. *Bioinformatics* **2002**, *18*, S22.
 (3) Kao-Huang, Y.; Revzin, A.; Butler, A. P.; O'Conner, P.; Noble, D. W.; von Hippel, P. H. *Proc. Natl. Acad. Sci. U.S.A.* **1977**, *74*, 4228.
 (4) Shimamoto, N. *J. Biol. Chem.* **1999**, *274*, 15293.
 (5) von Hippel, P. H.; Berg, O. G. *J. Biol. Chem.* **1989**, *264*, 675.
 (6) Halford, S. E.; Marko, J. F. *Nucleic Acids Res.* **2004**, *32*, 3040.
 (7) von Hippel, P. H.; Berg, O. G. *Proc. Natl. Acad. Sci. U.S.A.* **1986**, *83*, 1608.
 (8) von Hippel, P. H. *Science* **1994**, *263*, 769.
 (9) Bustin, M. *Mol. Cell. Biol.* **1999**, *19*, 5237.
 (10) Kornberg, R. D.; Lorch, Y. *Cell* **1999**, *98*, 285.

(11) Jen-Jacobson, L. *Biopolymers* **1997**, *44*, 153.
 (12) Johnson, J. D.; El-Bayoumi, M. A.; Weber, L. D.; Tulinsky, A. *Biochemistry* **1979**, *18*, 1292.
 (13) Edelman, G. M.; McClure, W. O. *Acc. Chem. Res.* **1968**, *1*, 65.
 (14) McClure, W. O.; Edelman, G. M. *Biochemistry* **1966**, *5*, 1908.
 (15) Wang, R.; Bright, F. V. *Appl. Spectrosc.* **1993**, *47*, 792.
 (16) Brand, L.; Gohlke, J. R. *Ann. Rev. Biochem.* **1972**, *41*, 843.
 (17) Allan, J.; Hartman, P. G.; Crane-Robinson, C.; Aviles, F. X. *Nature* **1980**, *288*, 675.
 (18) Cerf, C.; Lippens, G.; Muyldermans, S.; Segers, A.; Ramakrishnan, V.; Wodak, S. J.; Hallenga, K.; Wyns, L. *Biochemistry* **1993**, *32*, 11345.
 (19) Ramakrishnan, V. *Curr. Opin. Struct. Biol.* **1994**, *4*, 44.
 (20) DeToma, R. P.; Easter, J. H.; Brand, L. *J. Am. Chem. Soc.* **1976**, *98*, 5001.
 (21) Zhang, J.; Bright, F. V. *J. Phys. Chem.* **1991**, *95*, 7900.
 (22) Daniel, E.; Weber, G. *Biochemistry* **1966**, *5*, 1893.
 (23) Weber, L. D.; Tulinsky, A.; Johnson, J. D.; El-Bayoumi, M. A. *Biochemistry* **1979**, *18*, 1297.
 (24) McClure, W. O.; Edelman, G. M. *Biochemistry* **1967**, *6*, 559.

The CHT protein, isolated from bovine pancreas, is in a class of digestive enzymes and has the biological function of hydrolyzing polypeptide chains. However, physiological activity is determined by pH: at low pH, it is inactive, whereas at high pH, it becomes active.^{26,27} Several lines of evidence support that TNS is bound to CHT at some site other than the hydrophobic portion of the active site.^{13,24} However, the possibility of multiple binding sites of TNS to CHT cannot be ruled out.^{15,28} The binding structure of the protein–DNA complex was examined by the local orientational motion of the TNS probe. We found that the noncovalently bound TNS is displaced from the protein on interaction with DNA, elucidating the stronger interaction of CHT–DNA relative to that of TNS–CHT. Another fluorescent probe, ANS that binds rigidly at a single site on the surface of CHT, was similarly used to investigate nonspecific protein–DNA interactions. In contrast to the TNS–CHT–DNA complex in which the TNS probe gets displaced from its binding site on addition of DNA, the ANS–CHT–DNA complex is found to be frozen, revealing the very rigid structure at the recognition site. The dynamic rigidity of the ANS–CHT–DNA complex has enabled us to carry out Förster resonance energy transfer (FRET) studies from the donor (ANS–CHT–DNA complex) to another dye (acceptor), ethidium bromide (EB), intercalated in the genomic DNA. We also studied the enzymatic activity of CHT in the presence and absence of DNA and found the activity of the enzyme to be exactly the same in both cases, indicating that DNA nonspecifically binds to a site of CHT, which is away from its catalytic center. The structural integrity of the CHT protein upon complexation with DNA is confirmed by circular dichroism (CD) studies. Our steady-state and picosecond-resolved studies demonstrate unambiguously that TNS binds to multiple sites in CHT, in contrast to the single-site binding of ANS to the CHT enzyme.

Materials and Methods

Bovine pancreatic α -chymotrypsin (CHT), human serum albumin (HSA), 2,6-*p*-toluidinonaphthalene sulfonate (TNS), 1-anilinonaphthalene-8-sulfonate (ANS), Ala–Ala–Phe 7-amido-4-methyl coumarin (AAF-AMC), DNA (from salmon testes, sodium salt), sodium monophosphate, and sodium diphosphate were from Sigma Chemicals. Ethidium bromide (EB) was from Molecular Probes. The chemicals and the proteins are of the highest commercially available purity and were used as received. All aqueous solutions were prepared in phosphate buffer (10 mM, pH 7.4) using distilled water from a Millipore system. The TNS–CHT (or ANS–CHT) complexes were prepared by the mixing of TNS (or ANS), having a final concentration of 20 μ M with CHT (final concentration, 200 μ M). In this study, we considered the concentration of base pairs (bp) of the DNA to be the overall concentration of DNA. The procedure of preparing an aqueous solution of DNA and the measurement of DNA concentration are detailed in our previous work.²⁹ The total concentration of DNA in the aqueous solution was 200 μ M. The molar ratio of EB/DNA was maintained at 1:10 in the energy-transfer studies. It was shown previously that the molar ratio of 1:10 sufficed for EB for intercalative DNA binding, with the inter-EB distance determined to be 34 Å.²⁹ Catalytic measurements of CHT were made using the AAF-AMC substrate. The extinction coefficient used for determining the concentration of AAF-AMC in the buffer (10 mM, pH 7.4) is 16 mM⁻¹ cm⁻¹ at 325 nm.³⁰ For the enzymatic kinetics experiment, the enzyme concentration was

maintained at 20 μ M whereas that of the substrate was maintained at 200 μ M. The rate of formation of product was monitored using the change in absorbance at 370 nm of the product with time.

Steady-state absorption and emission were measured with a Shimadzu model UV-2450 spectrophotometer and a Jobin Yvon model Fluoromax-3 fluorimeter, respectively. Circular dichroism (CD) was performed with a model J-815 spectropolarimeter from Jasco using a 0.1 cm path length quartz cell. All experiments were done at room temperature (298 \pm 1 K). The fluorescence transients were taken with the use of the picosecond-resolved time-correlated single-photon counting (TCSPC) technique. We used a commercially available picosecond diode laser-pumped time-resolved fluorescence spectrophotometer from Edinburgh Instruments (LifeSpec-ps, U.K., excitation at 375 nm, instrument response function (IRF) of 80 ps). The fluorescence from the sample was detected by a microchannel plate photomultiplier tube (MCP–PMT) after dispersion through a monochromator. For all transients, the polarizer on the emission side was adjusted to 55° (magic angle) with respect to the polarization axis of the excitation beam. The observed fluorescence transients were fitted by using a nonlinear least-squares fitting procedure to a function ($X(t) = \int_0^t E(t') R(t-t') dt'$) composed of the convolution of the IRF ($E(t)$) with a sum of exponentials ($R(t) = A + \sum_{i=1}^N B_i e^{-t/\tau_i}$) with preexponential factors (B_i), characteristic lifetimes (τ_i), and a background (A). Relative concentration in a multiexponential decay was finally expressed as

$$c_n = \frac{B_n}{\sum_{i=1}^N B_i} \times 100$$

For temporal fluorescence anisotropy measurements, emission polarization was adjusted to be parallel or perpendicular to that of the excitation, and anisotropy was defined as $r(t) = [I_{\text{para}} - GI_{\text{perp}}] / [I_{\text{para}} + 2GI_{\text{perp}}]$. The magnitude of G , the grating factor of the emission monochromator of the TCSPC system, was found by the longtime tail matching technique to be 1.1.³¹

To estimate the fluorescence resonance energy transfer efficiency of the donor and hence to determine the distance of the donor–acceptor pair, we followed the methodology described in chapter 13 of ref 32. The Förster distance (R_0) is given by

$$R_0 = 0.211[\kappa^2 n^{-4} Q_D J(\lambda)]^{1/6} \text{ (in \AA)} \quad (1)$$

where κ^2 is a factor describing the relative orientation in space of the transition dipoles of the donor and acceptor. For donors and acceptors that randomize by rotational diffusion prior to energy transfer, the magnitude of κ^2 is assumed to be $2/3$. In the present study, the same assumption has been made. As discussed in ref 32, the choice of the κ^2 value is not crucial in the estimation of the donor–acceptor distance by using the FRET technique. For example, variations of the κ^2 value from 1 to 4 result in only a 26% change in the donor–acceptor distance. The implicit value of the refractive index (n) of the aqueous sample solutions is assumed to be 1.4. Q_D , the quantum yield of the donor (ANS–CHT–DNA) in the absence of an acceptor, is measured to be 0.041. $J(\lambda)$, the overlap integral, which expresses the degree of spectral overlap between the donor emission and the acceptor absorption, is given by

$$J(\lambda) = \frac{\int_0^\infty F_D(\lambda) \epsilon(\lambda) \lambda^4 d\lambda}{\int_0^\infty F_D(\lambda) d\lambda} \quad (2)$$

(25) Das, K.; Sarkar, N.; Bhattacharyya, K. *J. Chem. Soc., Faraday Trans.* **1993**, *89*, 1959.

(26) Zubay, G. *Biochemistry*; Addison-Wesley: Reading, MA, 1983; Chapter 4, p 130.

(27) Charman, W. N.; Porter, C. J. H.; Mithani, S.; Dressman, J. B. *J. Pharma. Sci.* **1997**, *86*, 269.

(28) Zhong, D.; Pal, S. K.; Zewail, A. H. *ChemPhysChem* **2001**, *2*, 219.

(29) Sarkar, R.; Pal, S. K. *Biopolymers* **2006**, *83*, 675.

(30) Kamal, J. K. A.; Xia, T.; Pal, S. K.; Zhao, L.; Zewail, A. H. *Chem. Phys. Lett.* **2004**, *387*, 209.

(31) O'Connor, D. V.; Philips, D. *Time Correlated Single Photon Counting*; Academic Press: London, 1984.

(32) Lakowicz, J. R. *Principles of Fluorescence Spectroscopy*; Kluwer Academic/Plenum: New York, 1999.

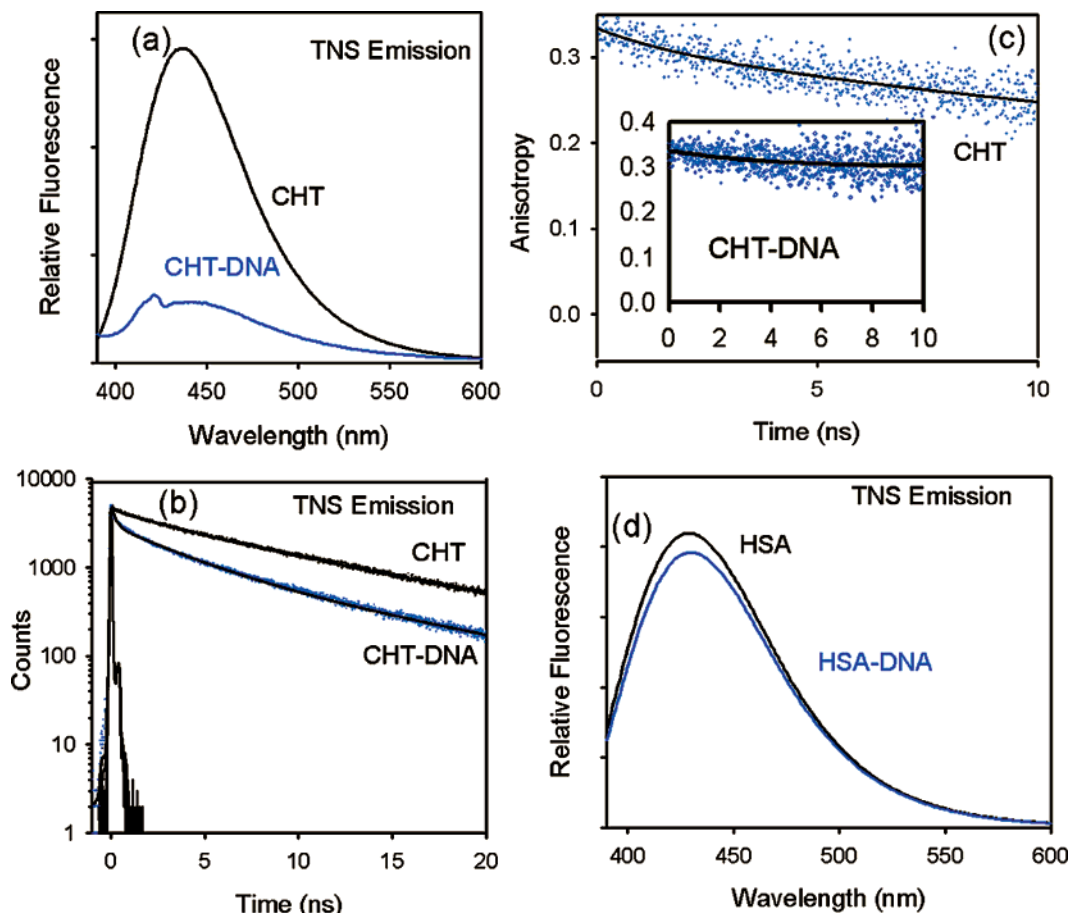


Figure 1. (a) Steady-state fluorescence spectra of TNS bound to CHT in the presence and absence of salmon sperm DNA (SS DNA). (b) Time-resolved transients of TNS bound to CHT in the presence and absence of SS DNA. (c) Time-resolved anisotropy of TNS bound to CHT in the absence of DNA. The inset shows the time-resolved anisotropy of TNS bound to CHT in the presence of DNA. (d) Steady-state fluorescence spectra of TNS bound to HSA in the presence and absence of SS DNA.

where $F_D(\lambda)$ is the fluorescence intensity of the donor in the wavelength range of λ to $\lambda + d\lambda$ and is dimensionless. $\epsilon(\lambda)$ is the extinction coefficient (in $M^{-1} \text{ cm}^{-1}$) of the acceptor at λ . If λ is in nm, then $J(\lambda)$ is in units of $M^{-1} \text{ cm}^{-1} \text{ nm}^4$. Once the value of R_0 is known, the donor-acceptor distance (r) can easily be calculated by using the equation

$$r^6 = \frac{R_0^6(1-E)}{E} \quad (3)$$

Here, E is the efficiency of energy transfer. The transfer efficiency is measured by using the relative fluorescence intensity of the donor in the absence (F_D) and presence (F_{DA}) of the acceptor. The efficiency E is also calculated from the lifetimes under these respective conditions (τ_D and τ_{DA}).

$$E = 1 - \left(\frac{F_{DA}}{F_D} \right) \quad (4a)$$

$$E = 1 - \left(\frac{\tau_{DA}}{\tau_D} \right) \quad (4b)$$

The distances measured with eqs 4a and 4b are revealed as R^S (steady-state measurement) and R^{TR} (time-resolved measurement), respectively.

Results and Discussion

TNS, one of the most popular biological probes, exhibits great sensitivity to its local environment as a consequence of the significant difference between its excited- and ground-state dipole

moments,^{33,34} which strongly affects the spectral, temporal, and polarization characteristics.³² It has been proposed by several groups that the TNS fluorescence observed in protein solutions results from the binding of the fluorophore to hydrophobic sites at the protein surface^{14,22,35,36} and perhaps increased environmental rigidity.^{37,38} Despite its widespread use as a probe of macromolecular structures, the nature of the sites where TNS binds and the forces governing this binding are not well defined. Hydrophobic interaction between TNS and low-polarity regions of the target structure is often suggested to play a major role in the binding of TNS, but there are indications that electrostatic interactions may also be significant.³⁹ Experiments have been carried out that provide evidence for the existence of a site in the CHT protein that has a high affinity for TNS but is not part of the enzyme active site.²⁴ Apparently, the affinity of the active site of CHT for TNS is considerably less than that of a second hydrophobic region.

In an aqueous solution, the emission quantum yield of TNS is very small (0.001)⁴⁰ with an emission maximum at 500 nm and a very short lifetime of 60 ps.²⁸ The emission intensity, maximum, and lifetime of TNS remain unchanged in phosphate

(33) Seliskar, C. J.; Brand, L. *J. Am. Chem. Soc.* **1971**, *93*, 5414.

(34) Greene, F. C. *Biochemistry* **1975**, *14*, 747.

(35) Stryer, L. *J. Mol. Biol.* **1965**, *13*, 482.

(36) Turner, D. C.; Brand, L. *Biochemistry* **1968**, *7*, 3381.

(37) Penzer, G. R. *Eur. J. Biochem.* **1972**, *25*, 218.

(38) Ainsworth, S.; Flanagan, M. T. *Biochim. Biophys. Acta* **1969**, *194*, 213.

(39) Flanagan, M. T.; Ainsworth, S. *Biochim. Biophys. Acta* **1968**, *168*, 16.

(40) Datta, A.; Mandal, D.; Pal, S. K.; Das, D.; Bhattacharyya, K. *J. Chem. Soc., Faraday Trans.* **1998**, *94*, 3471.

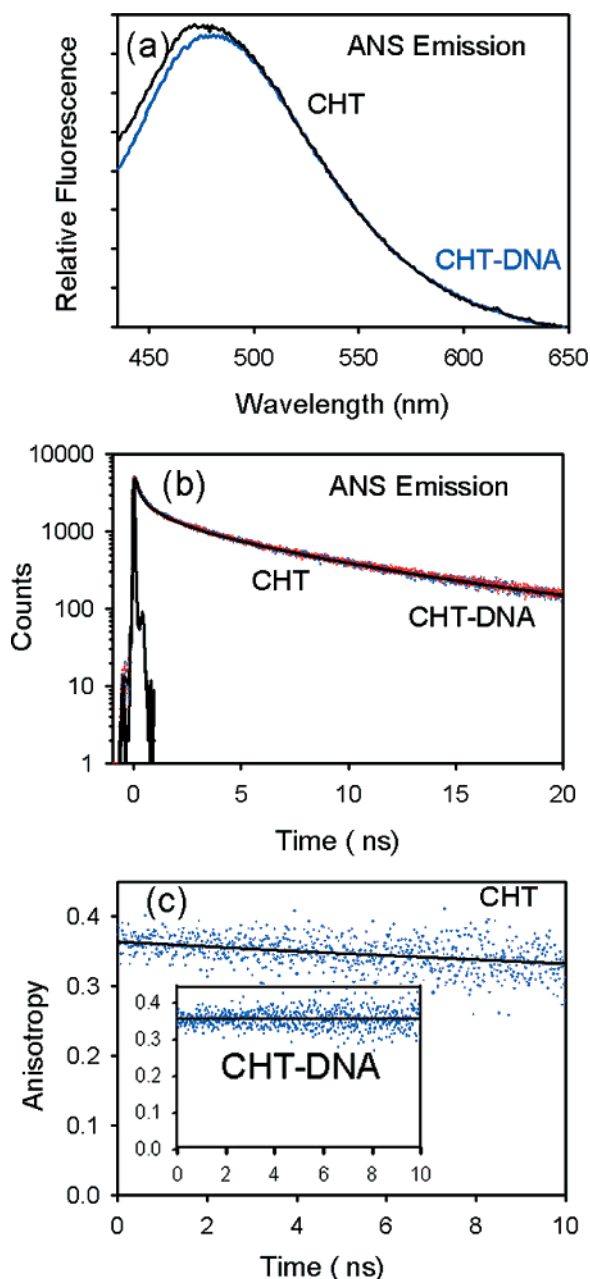


Figure 2. (a) Steady-state fluorescence spectra of ANS bound to CHT in the presence and absence of SS DNA. (b) Time-resolved transients of ANS bound to CHT in the presence and absence of SS DNA. (c) Time-resolved anisotropy of ANS bound to CHT in the absence of DNA. The inset shows the time-resolved anisotropy of ANS bound to CHT in presence of DNA.

buffer (10 mM, pH 7.4) compared to those in pure water. Figure 1a presents the steady-state fluorescence spectrum of a TNS–CHT aqueous solution, which displays a large relative fluorescence intensity together with a blue shift of 65 nm compared to that in buffer (500 nm). When measured in protein solutions, the quantum yield of TNS dramatically increases (0.18^{13}) as a result of the attachment of TNS to the protein. Upon addition of DNA to TNS–CHT aqueous solution, we found a considerable decrease in the fluorescence emission together with a peak shift to the red by 10 nm, from 435 nm in TNS–CHT to 445 nm (Figure 1a). The quenching of the steady-state fluorescence intensity of the TNS–CHT–DNA complex together with the red shift compared to that of TNS–CHT indicates that DNA repels TNS out of the binding sites of CHT into the vicinity of the polar aqueous medium. Figure 1b shows picosecond-resolved transients of CHT-

bound TNS and as a complex with DNA. The decays are found to be multiexponential in nature with three decay components (τ_i) and their corresponding preexponential factors (a_i). For the TNS–CHT complex (Figure 1b, emission at 435 nm), the overall fluorescence decay leads to an average decay time ($\sum a_i \tau_i$) constant of 9.87 ns. The fluorescence transient of the TNS–CHT–DNA complex (emission at 445 nm) is found to be (Figure 1b) faster (average decay time of 7.75 ns) than that of the CHT-bound TNS emission. The faster fluorescence decay along with the reduced quantum yield of TNS–CHT in the presence of DNA also indicates the expulsion of TNS from its stronger binding sites to the proximity of bulk water. We expect that the formation of a nonspecific protein–DNA complex arises as a result of the electrostatic interaction between the randomly distributed charges on the surface of the protein with the DNA. Thus, the above-described steady-state and time-resolved studies indicate that the surface–surface electrostatic interaction between the DNA and the CHT protein is much stronger than the point-surface contact of TNS with CHT.

To probe the local rigidity of the TNS–CHT complex, we measured the time-resolved anisotropy (Figure 1c) of TNS at the peak emission of 435 nm. The fluorescence anisotropy decay of TNS bound to CHT reveals two decay components: a faster component of 2.0 ns (8.2%) and a slower component of 47 ns (91.8%). The faster time constant corresponds to the local reorientational motion of the probe. The major contribution of the slower component of 47 ns, which corresponds to a global tumbling motion of the CHT protein,^{41,42} reflects the rigidity of the TNS at the binding site of CHT. However, the anisotropy decay (at 445 nm) of the TNS–CHT–DNA complex (inset of Figure 1c) revealed significantly large residual anisotropy (90%), which does not decay within our experimental time window. This observation is consistent with the fact that most of the TNS molecules get displaced from stronger binding sites of CHT upon complexation with DNA in the vicinity of bulk water, which is expected to show 75 ps²⁸ $r(t)$ decay dynamics and is not evident in our measurement (IRF = 80 ps). However, the TNS molecules, which remain with CHT even upon complexation with DNA, show more dynamical restriction on the rotational motion of CHT in the CHT–DNA complex. An increase in the steady-state anisotropy value (data not shown) of TNS–CHT upon complexation with DNA (from 0.28 to 0.38) also supports the above argument. It also has to be noted that at the wavelength of the anisotropy measurement on the TNS–CHT–DNA complex (at 445 nm) the contribution from the fluorescence intensity of rigidly bound TNS molecules (quantum yield = 0.18^{13}) is higher than that of the displaced TNS (quantum yield = 0.001^{40}) in the vicinity of the bulk water.

We also studied the interaction of the TNS probe with another protein, human serum albumin (HSA), that recognizes a wide variety of agents and transports them in the bloodstream.⁴³ HSA contains several hydrophobic cavities where drug and surfactant molecules can bind. According to crystallographic studies, HSA consists of three domains, I, II, and III, each of which are subdivided into two subdomains, A and B. Using X-ray crystallography, He and Carter studied the binding of several drug molecules to HSA.⁴⁴ The principal regions of ligand binding to HSA are located in hydrophobic cavities in subdomains IIA (binding site I) and IIIA (binding site II). Figure 1d presents the

(41) Shaw, A. K.; Sarkar, R.; Banerjee, D.; Hintschich, S.; Monkman, A.; Pal, S. K. *J. Photochem. Photobiol., A* **2007**, *185*, 76.

(42) Taran, V. N. D.; Veeger, C.; Visser, A. J. *Eur. J. Biochem.* **1993**, *211*, 47.

(43) Berde, C. B.; Hudson, B. S.; Simoni, R. D.; Sklar, L. A. *J. Biol. Chem.* **1979**, *254*, 391.

(44) He, X. M.; Carter, D. C. *Nature* **1992**, *358*, 209.

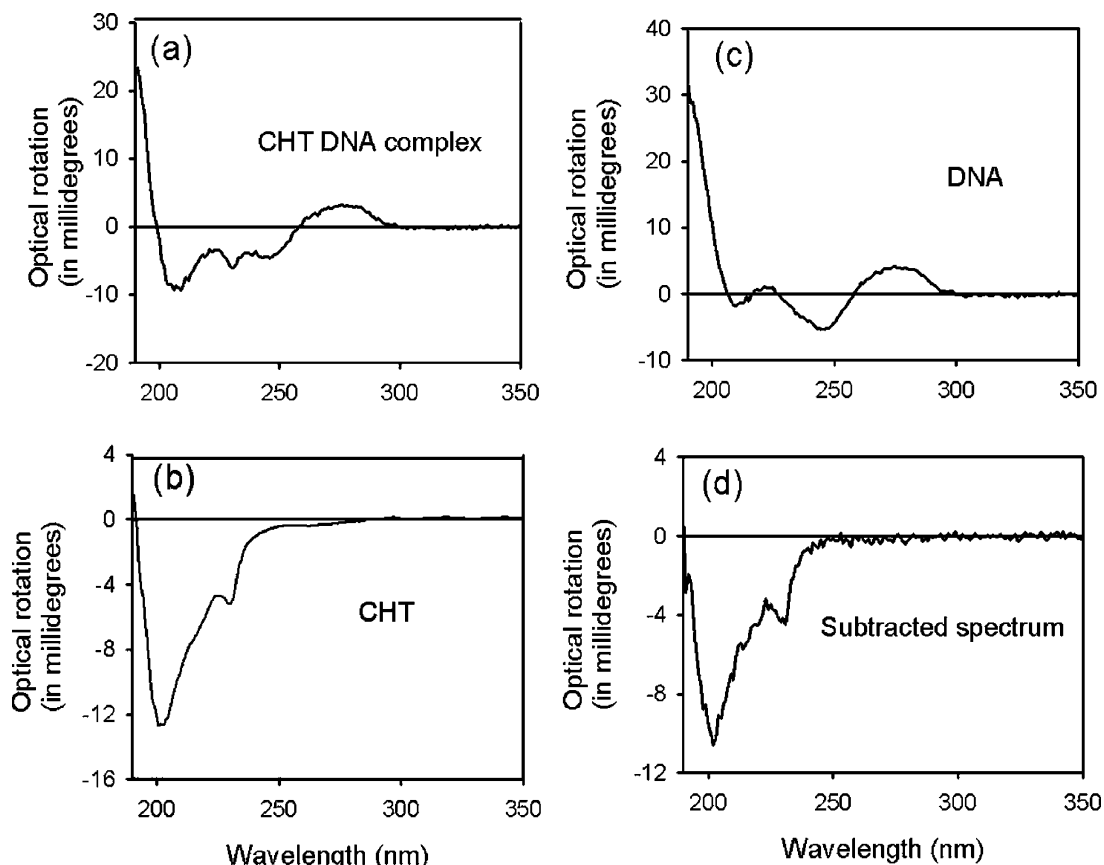


Figure 3. Circular dichroism (CD) spectra of (a) the CHT–DNA complex, (b) the CHT enzyme, and (c) the salmon sperm DNA. (d) Spectrum obtained by subtraction of the DNA spectra from that of the CHT–DNA complex to show the structural integrity of CHT in the complex.

steady-state fluorescence spectrum of TNS–HSA and upon complexation with DNA. As obvious from Figure 1d, upon addition of DNA to the TNS–HSA aqueous solution we found no change in the steady-state emission intensity, which indicates that TNS rigidly binds to the hydrophobic cavities of HSA, which DNA cannot access. We also found the picosecond-resolved transients of TNS–HSA to be exactly the same as that of its complex with DNA (data not shown). This observation is consistent with the fact that TNS binds to HSA in a deep hydrophobic cavity, in contrast to the surface binding of TNS in CHT. However, the fluorescence anisotropy of TNS-labeled HSA in the presence of DNA has a relatively higher residual anisotropy value (data not shown) compared to that of TNS–HSA, reflecting the considerable interaction of the protein with DNA.

Interactions of CHT-bound ANS with SS DNA are shown in Figure 2. An extensive fluorescence study¹² followed by an X-ray study²³ on the ANS–CHT complex indicated that ANS binds rigidly at a single site on the surface of the protein near the Cys-1-122 disulfide bond. This ANS binding site is almost diametrically opposite in position to the enzymatic center. In Figure 2a, we present the steady-state fluorescence spectra of CHT-bound ANS and its complex with DNA. The emission intensity of ANS–CHT is observed to be similar to that of the ANS–CHT–DNA complex, revealing the fact that ANS molecules are not detached from CHT upon complexation. The time-resolved studies (Figure 2b) also confirm the above results. The time-resolved anisotropy decay (at 480 nm) of ANS–CHT, shown in Figure 2c, revealed a rotational time constant of 47 ns attributed to the global tumbling motion of the CHT protein.^{41,42} However, the $r(t)$ decay of the ANS–CHT–DNA complex (inset in Figure 2c) exhibited a very long time component with a

significantly large residual anisotropy (residual $r(t)$), which does not decay within our experimental time window. The above results confirm the rigidity of the ANS–CHT complex and the suppression of CHT motion in the CHT–DNA complex. An increase in the steady-state anisotropy value (data not shown) of ANS–CHT upon complexation with DNA (from 0.26 to 0.37) is in agreement with the above conclusion. To investigate the possibility of any structural perturbation of CHT upon complexation with DNA, we carried out circular dichroism (CD) studies. As evident by comparison of Figure 3, the CD spectrum of CHT in bulk water remains essentially similar to that in the presence of DNA.

The intactness of the interaction of ANS with CHT upon complexation with DNA offers the opportunity to estimate the distance of the DNA contact point from the well-defined ANS binding site in CHT. In this regard, we label DNA with ethidium bromide (EB). Ethidium bromide (EB) is a well-known fluorescent probe for DNA, which readily intercalates into the DNA double helix.^{45,46} Compared to the case of bulk water, the emission intensity and lifetime of EB increase nearly 11 times when EB intercalates into the double helix of DNA.⁴⁷ This remarkable fluorescence enhancement of EB is utilized to study the motion of DNA segments. The photophysical processes of the EB fluorescence enhancement have also been explored.⁴⁷ The significantly large spectral overlap of the donor (ANS) emission and acceptor (EB) absorption spectra together with the close proximity of acceptor and donor favors energy transfer from the

(45) Fiebig, T.; Wan, C.; Kelley, S. O.; Barton, J. K.; Zewail, A. H. *Proc. Natl. Acad. Sci.* **1999**, *96*, 1187.

(46) Millar, D. P.; Robbins, R. J.; Zewail, A. H. *J. Chem. Phys.* **1982**, *76*, 2080.

(47) Pal, S. K.; Mandal, D.; Bhattacharyya, K. *J. Phys. Chem. B* **1998**, *102*, 11017.

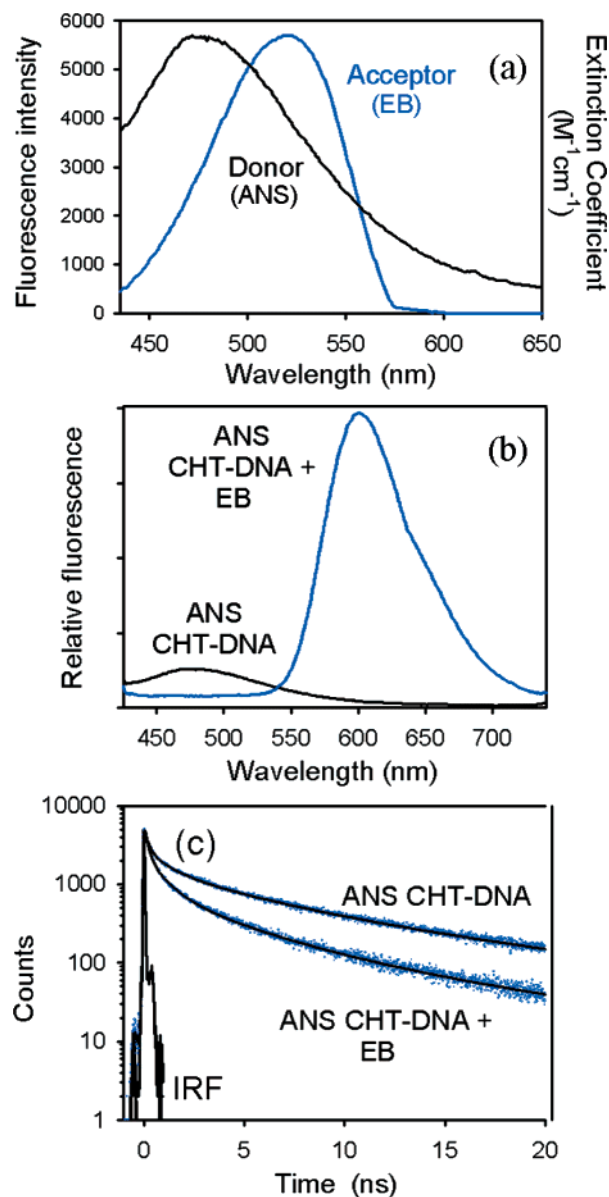


Figure 4. (a) Spectral overlap between donor (ANS–CHT–DNA complex) emission and acceptor (ANS–CHT with EB-bound DNA) absorbance. (b) Steady-state fluorescence quenching of the donor (ANS–CHT–DNA complex) in the presence of the acceptor, ethidium bromide (EB), in DNA. (c) Picosecond-resolved transients of the donor (ANS–CHT–DNA complex) in the absence and presence of the acceptor (EB) in DNA.

donor to the acceptor. The spectral overlap of the donor (ANS–CHT–DNA complex) emission and the acceptor (ANS–CHT with EB-labeled DNA) absorption spectra is shown in Figure 4a. As clearly evident from the steady-state fluorescence spectrum (Figure 4b), the emission intensity of the donor is quenched on inclusion of the acceptor (EB) in the DNA. The time-resolved studies also confirm the energy-transfer process (Figure 4c). The picosecond-resolved transient (Figure 4c) of the donor reveals an average decay time constant of 0.88 ns as compared to 0.54 ns for the donor in the presence of the acceptor. The drop in the average decay time of the donor–acceptor complex compared to that of the donor alone also confirms that energy transfer occurs from ANS to EB as a result of dipolar coupling. The calculated (from eqs 4a and 4b) donor-to-acceptor energy-transfer efficiency from steady-state and time-resolved studies are 39.6 and 34.1%, respectively. The estimated donor–acceptor distances from steady-state and time-resolved experiments are 22.9 and

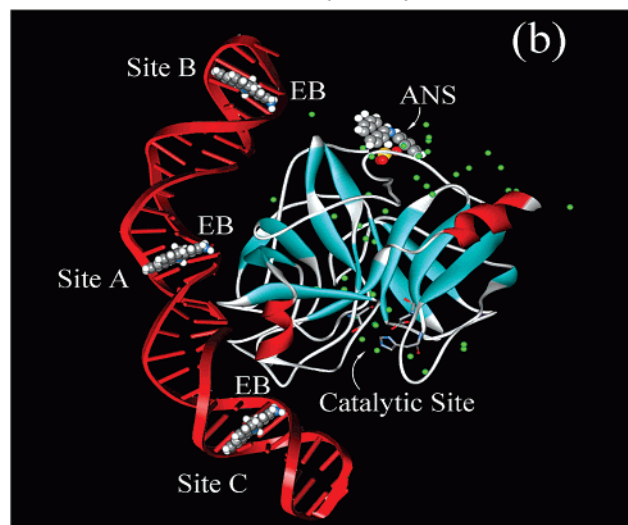
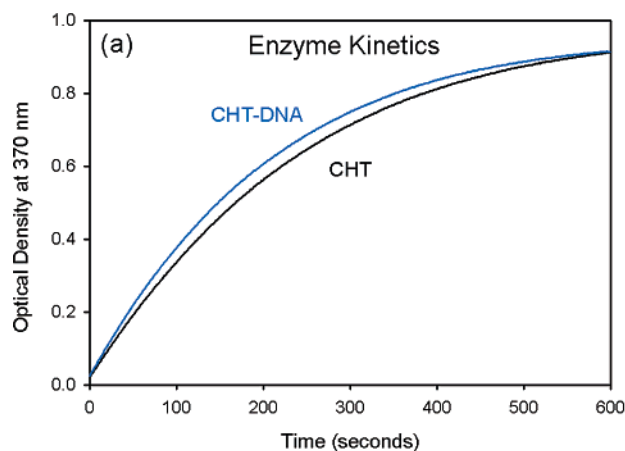


Figure 5. (a) Enzymatic activity of CHT on the substrate, AAF–AMC, in the presence and absence of SS DNA. (b) Schematic representation of nonspecific protein–DNA binding interactions. The spheres indicate the water molecules observed in an X-ray crystallographic study²³ on the CHT enzyme. (See the text.)

23.8 Å, respectively. It should be noted that the ANS binding site and the enzymatic active site of CHT are at almost diametrically opposite points.²³ The estimated distance between the above two sites is ~40 Å. Our measurement of the ANS–EB distance of ~23.5 Å reveals that DNA interacts with CHT at a site that is located between the ANS binding site and the enzymatic active site of CHT. To investigate the proximity of the DNA surface to the active site of the CHT enzyme, we measured the enzymatic activity of CHT upon complexation with DNA. Figure 5a shows the rate of formation of the AMC product with respect to the enzymatic activity of CHT on AAF–AMC. It is clearly evident from the Figure 5a that the activity of the enzyme remains almost unaffected in the presence of the DNA. This observation is consistent with the fact that the active site of CHT in the CHT–DNA complex is completely available to the substrate of the enzyme. The nature of the CHT–DNA complex is shown in a schematic (Figure 5b). In the experiment, we have maintained the [DNA]/[EB] ratio in such a way that the distance between two EBs is expected to be 34 Å (10 bp).²⁹ As shown in Figure 5b, the measured ANS–EB distance (23.5 Å) could be the average distance from ANS to EB at sites A and B. The energy transfer from ANS due to dipolar coupling to a distant EB at site C is forbidden.

Conclusions

Nonspecific protein–DNA interactions of a CHT enzyme protein with genomic DNA reveal the nature of ligand binding of the protein in aqueous solution. The TNS probe has been found to bind CHT at a site different from the active site of the enzyme, mostly to the positively charged basic residues at the surface sites of the protein. The possibility of TNS binding to the hydrophobic cavities/clefts cannot be ruled out. Steady-state and picosecond-resolved fluorescence studies reveal the displacement of TNS from TNS-labeled CHT upon complexation with DNA. The observations are consistent with the surface binding of TNS to CHT. The steady-state and time-resolved emission of TNS in CHT upon complexation with DNA also suggests multiple binding sites of TNS to CHT. As a control study, we also investigated the binding of TNS to HSA, in which the TNS probe can bind to the deep hydrophobic cavity of the protein. The complexation of HSA with DNA reveals no displacement of the ligand probes from the protein. However, fluorescence anisotropy studies confirm the complexation of HSA

with DNA. Thus, nonspecific protein–DNA interaction studies are relevant to investigations of the nature of ligand binding to a particular protein. Studies on ANS-labeled CHT upon complexation with DNA show that DNA does not interact with CHT through the well-defined ANS binding site. The studies also offer the opportunity to measure the average distance between the well-defined ANS binding site and the EB-labeled DNA surface in the vicinity of CHT. An investigation of the enzymatic activity of CHT upon complexation with DNA clearly rules out the blocking of the active site of CHT as a result of the proximity of the DNA surface. Circular dichroism (CD) studies on the free protein in buffer and as a complex with DNA confirm the structural integrity of CHT in the protein–DNA complex. Our studies on the nonspecific protein–DNA interaction may find its future importance in the investigation of ligand binding sites of proteins.

Acknowledgment. S.S.N. thanks CSIR for a fellowship. We thank DST for a financial grant (SR/FTP/PS-05/2004).

LA063586X